

Complex Langevin for Lattice QCD

D. K. Sinclair*

HEP Division, Argonne National Laboratory, 9700 South Cass Avenue, Argonne, Illinois 60439, USA

E-mail: dks@hep.anl.gov

J. B. Kogut

Department of Energy, Division of High Energy Physics, Washington, DC 20585, USA and

Department of Physics – TQHN, University of Maryland, 82 Regents Drive, College Park, MD 20742, USA

E-mail: jbkogut@umd.edu

We simulate lattice QCD at finite quark-number chemical potential, μ , using the complex-Langevin equation (CLE) with gauge-cooling and adaptive updating to prevent instabilities. The CLE is used because QCD at finite μ has a complex fermion determinant which precludes the use of standard simulation methods based on importance sampling. Since, even when CLE simulations converge, they are not guaranteed to produce correct results except under very stringent conditions, which lattice QCD at finite μ does not obey, we need extensive testing to determine under what conditions it produces reliable results. We performed simulations at $\beta = 6/g^2 = 5.6$ and $\beta = 5.7$, both at m = 0.025. For small μ and μ large enough to produce saturation, measured observables appear to be approaching their correct values as the coupling is decreased. However, for intermediate μ values, these simulations predict a transition from hadronic to nuclear matter at a μ which is far too small. Since there is evidence that for CLE simulations to produce correct results the trajectories should remain close to the SU(3) manifold (at least for small μ), we explore the parameter space to see where this is true. We find that the distance from this manifold decreases as the coupling decreases and as the quark mass (in lattice units) decreases, i.e. as we approach the continuum limit. This indicates that we need to simulate at smaller couplings and quark masses (requiring larger lattices) to see if these can produce the correct physics.

The 36th Annual International Symposium on Lattice Field Theory - LATTICE2018 22-28 July, 2018

Michigan State University, East Lansing, Michigan, USA.

^{*}Speaker.

[†]This research was supported in part by US Department of Energy contract DE-AC02-06CH11357

1. Introduction

QCD at finite quark/baryon-number density describes nuclear matter, the constituent of the interiors of neutron stars and heavy nuclei. Hot nuclear matter is produced in relativistic heavy-ion colliders, and was present in the early universe.

QCD at finite baryon/quark-number density has a sign problem which prevents direct application of standard lattice simulations that are based on importance sampling. When finite density is implemented by introducing a quark-number chemical potential μ , the sign problem manifests itself by making the fermion determinant complex. This precludes the direct application of standard lattice QCD simulations based on importance sampling. Since Langevin simulations are not based on importance sampling, they can be extended to the case of complex actions [1, 2, 3, 4]. For lattice QCD this requires analytically continuing the gauge fields from SU(3) to SL(3,C). Complex Langevin (CLE) simulations cannot be guaranteed to produce correct results unless the trajectories are restricted to a compact domain, the drift term is holomorphic in the fields and the solutions are ergodic [5, 6, 7, 8, 9, 10, 11, 12]. However, zeroes of the fermion determinant produce poles in the drift term making it meromorphic not holomorphic in the fields. Thus convergence to the correct limits cannot be guaranteed. CLE simulations of lattice QCD at finite μ with heavy quarks have been performed by [13, 14, 15, 16, 17]. CLE simulations with lighter quarks have been performed by [18, 15, 19, 20, 21]. For a good summary of recent work on applying the CLE to lattice QCD at finite μ with a guide to the literature see [10].

Our investigations [22] are aimed at determining whether the CLE is a viable way of simulating QCD at finite μ , and if so, under what conditions. We have performed CLE simulations of lattice QCD at zero temperature and μ s ranging from zero to saturation, at $\beta = 6/g^2 = 5.6$ and $\beta = 5.7$, both at m = 0.025 The weaker coupling shows good agreement with expectations at small and large μ s, but fails for couplings in the transition region. The results are compared with those of the phase-quenched approximation, since random matrix theory suggests that when the CLE fails, it produces phase-quenched results [23]. Other random matrix CLE simulations seem more optimistic [24] In addition full and phase-quenched simulations are expected to agree at small and large μ .

Since it appears that good results might be obtained with the CLE if the trajectories remain close to the SU(3) manifold, we are studying how the unitarity norm, which measures this closeness, depends on quark mass (m) and β . We find that the average distance from this manifold decreases as m decreases and as the coupling g decreases (β increases), i.e. as we approach the continuum limit.

2. Complex Langevin Equation for Lattice QCD at finite μ

If S(U) is the gauge action after integrating out the quark fields, The Langevin equation for the evolution of the gauge fields U in Langevin time t is:

$$-i\left(\frac{d}{dt}U_l\right)U_l^{-1} = -i\frac{\delta}{\delta U_l}S(U) + \eta_l$$
 (2.1)

where S(U) is the gauge action after integrating out the quark fields. l labels the links of the lattice, and $\eta_l = \eta_l^a \lambda^a$. Here λ_a are the Gell-Mann matrices for SU(3) and $\eta_l^a(t)$ are Gaussian-distributed

random numbers normalized so that:

$$\langle \eta_{l}^{a}(t)\eta_{l'}^{b}(t')\rangle = \delta^{ab}\delta_{ll'}\delta(t-t') \tag{2.2}$$

The complex-Langevin equation has the same form except that the Us are now in SL(3,C). S, now $S(U,\mu)$ is

$$S(U,\mu) = \beta \sum_{\Box} \left\{ 1 - \frac{1}{6} Tr[UUUU + (UUUU)^{-1}] \right\} - \frac{N_f}{4} Tr\{ln[M(U,\mu)]\}$$
 (2.3)

where $M(U,\mu)$ is the staggered Dirac operator, backward links are represented by U^{-1} not U^{\dagger} and we choose to keep the noise term η real. We simulate the time evolution of the gauge fields using a partial second-order formalism, and stochastic estimators for $\text{Tr}\{ln[M]\}$ [26, 27, 28]

We apply adaptive updating: if the force term becomes too large, dt is decreased to keep it under control. After each update, we gauge cool [25], gauge fixing to the gauge which minimizes the unitarity norm:

$$F(U) = \frac{1}{4V} \sum_{x,\mu} Tr \left[U^{\dagger} U + (U^{\dagger} U)^{-1} - 2 \right] \ge 0.$$
 (2.4)

We use unimproved staggered quarks.

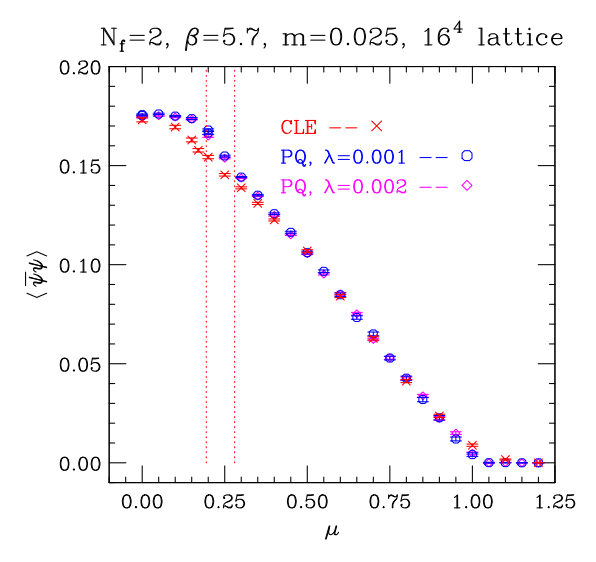
3. Zero Temperature Simulations at $\beta = 5.6$ and $\beta = 5.7$, m = 0.025

We perform CLE simulations of 2-flavour lattice QCD at zero temperature at $\beta = 5.6$, m = 0.025 on a 12⁴ lattice and at $\beta = 5.7$, m = 0.025 on a 16⁴ lattice from $\mu = 0$ up to saturation. For comparison, we perform RHMC simulations of the phase-quenched approximation over the same parameter range, since random matrix theory suggests that when the CLE simulations fail they produce the phase-quenched results.

The phase-quenched approximation is known to undergo a phase transition to a superfluid phase at $\mu \approx m_\pi/2$. The chiral condensate is constant up to this transition and decreases beyond it, vanishing at saturation. The quark-number density is zero up to the transition beyond which it rises up to saturation, where all states are filled (density=3 in our normalization). At saturation the quarks decouple and we have a pure gauge theory. For the full theory one expects the observables to remain at their $\mu=0$ values up to $\mu \approx m_N/3$ above which they evolve towards saturation. For $\beta=5.6$, m=0.025, $m_\pi/2\approx0.21$, $m_N/3\approx0.33$ [29], while for $\beta=5.7$, m=0.025, $m_\pi/2\approx0.194$, $m_N/3\approx0.28$ [30, 31]. We typically run for 2-3 million updates at each β and μ .

Figure 1 shows the chiral condensate $(\langle \bar{\psi}\psi \rangle)$, figure 2 the quark-number density and figure 3 the plaquettes, as functions of μ at $\beta=5.7$, m=0.025 on a 16^4 lattice. The vertical red dotted lines are at $\mu=m_\pi/2$ and $\mu=m_N/3$ respectively. For μ at or near zero and for μ at saturation, where the quarks decouple and the gauge fields exhibit pure gauge dynamics, these observables are in good agreement with known values, a considerable improvement from $\beta=5.6$. However, for both β s, these graphs show a transition from hadronic to nuclear matter at a $\mu < m_\pi/2$, rather than at $\mu \approx m_N/3$, a result even worse than the phase-quenched approximation.

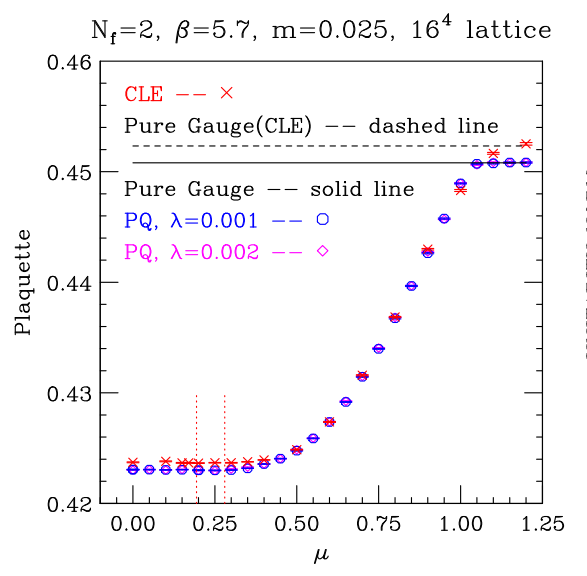
The unitarity norm is significantly greater than zero throughout the transition region for both β values, only becoming small around $\mu=0.5$. For $\beta=5.7$, it remains small through $\mu=0.8$ before increasing towards its pure gauge value at saturation. We conjecture that this means we can trust the CLE for $\mu \geq 0.5$.

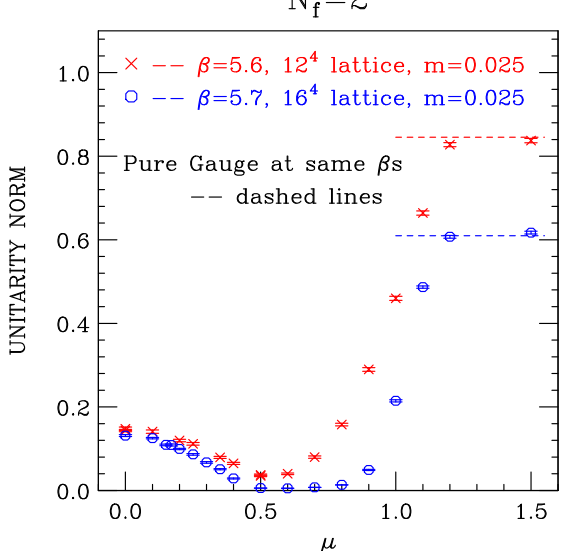


 $N_f = 2$, $\beta = 5.7$, m = 0.025, 16^4 lattice CLE -- \times PQ, λ=0.001 -- ○ 3 PQ, $\lambda = 0.002$ Quark Number Density 2 0.00 0.25 1.00 1.25 0.50

Figure 1: Chiral condensate as a function of μ on a 16⁴ lattice at $\beta = 5.7$ and m = 0.025.

Figure 2: Quark-number density as a function of μ on a 16⁴ lattice at $\beta = 5.7$ and m = 0.025.





tice at $\beta = 5.7$ and m = 0.025.

Figure 3: Plaquette as a function of μ on a 16⁴ lat- Figure 4: Average unitarity norm as a function of μ for $\beta = 5.6$, on a 12⁴ lattice – red, and for $\beta = 5.7$ on a 16⁴ lattice – blue.

4. Dependence of the Unitarity Norm on *m* and on $\beta = 6/g^2$

The behaviour of the CLE seems to improve if the gauge fields remain close to the SU(3)manifold, i.e. if the unitarity norm remains small. It is thus useful to study how the average unitarity norm depends on the simulation parameters. Therefore we study how this norm depends on m and β . Since we have seen that in the small μ regime ($\mu < 0.5$), where failures of the CLE first manifest themselves, the unitarity norm decreases as μ increases from zero, it will suffice to restrict ourselves to $\mu = 0$. With β fixed at 5.6 and $\mu = 0$, we determine the dependence of the unitarity norm on the quark mass m for $0.1 \le m \le \infty$. This dependence is shown in figure 5. The

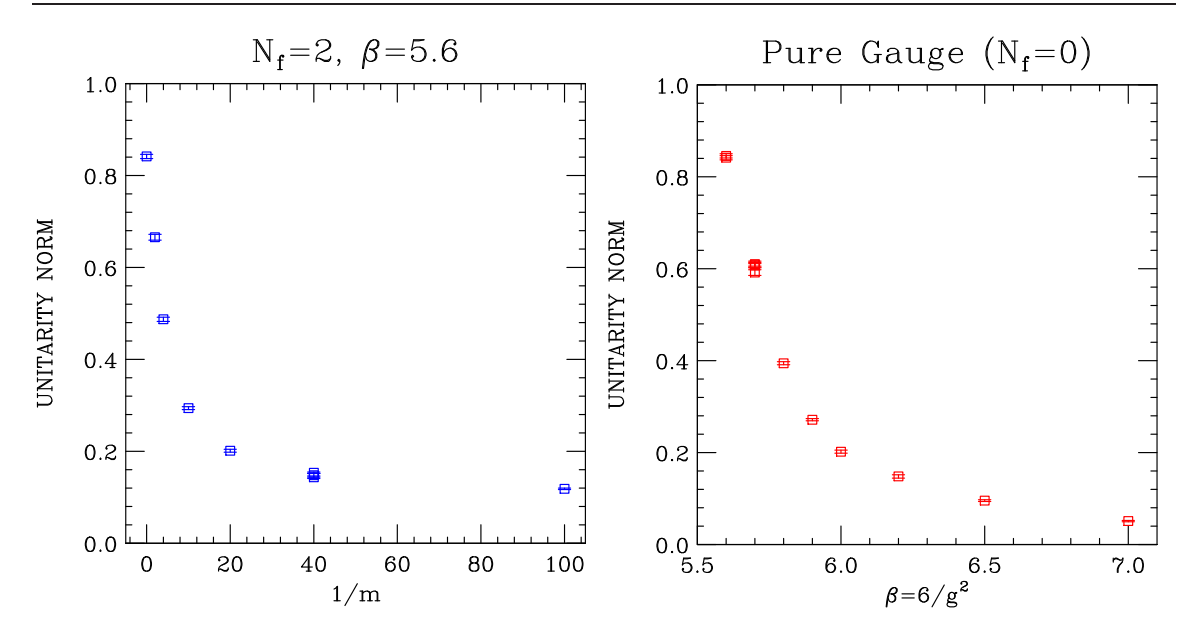


Figure 5: Unitarity norm as a function of inverse **Figure 6:** Unitarity norm as a function of $\beta = 6/g^2$ quark mass at $\beta = 5.6$ for pure SU(3) gauge theory.

unitarity norm decreases as m decreases falling by a factor of about 7 over this range.

We have already seen that, with m fixed at 0.025 the unitarity norm decreases when β is increased from 5.6 to 5.7. Since the unitarity norm has its maximum for $m = \infty$, i.e. for pure SU(3) Yang-Mills theory, we choose to apply the CLE for this mass. Because there are no quarks such simulations are cheap and can be performed on smaller lattices than for lighter quarks. In addition, without quarks, the action is holomorphic in the fields, so that provided that the regions over which they evolve are strongly bounded (and simply connected), the CLE should be valid. We have run CLE simulations for β s in the range $5.6 \le \beta \le 7.0$. The unitarity norms decrease as β is increased (g is decreased), falling by more than an order of magnitude over this range. This is shown in figure 6. Except at $\beta = 5.6$ the plaquette values are in excellent agreement with the exact (monte-carlo) results indicating that the CLE produces correct results. We note that our $\mu = 0$ simulations at $\beta = 5.8$, m = 0.02 and $\beta = 5.9$, m = 0.015 on a 32⁴ lattice give further indications that the unitarity norm decreases as β is increased and m is decreased.

The indications are that the unitarity norm will approach zero as m and g approach zero, i.e. in the continuum limit. This gives us hope that the CLE might deliver correct results in this limit.

5. Discussion and Conclusions

We have simulated 2-flavour lattice QCD at $\beta = 5.6$, m = 0.025 and $\beta = 5.7$, m = 0.025 from $\mu = 0$ to $\mu = 1.5$ (saturation) using the CLE with gauge-cooling and adaptive updating. These runs were performed on lattices which are (at least for small μ s) at zero temperature. For μ small, and for μ at saturation, the observables appear to approach their physical values as β is increased. At intermediate μ values the transition from hadronic to nuclear matter occurs at an unphysically small μ .

It has been observed that CLE simulations are more likely to give the correct results if the trajectories remain close to the SU(3) manifold. We study the dependence of the average distance

from this manifold on (lattice) quark mass m and on $\beta = 6/g^2$, and find that this decreases as m and g decrease, i.e. as the continuum limit is approached. This suggests that we might find correct physics, even in the transition region, for large enough β s and small enough ms. It remains an open question whether the continuum limit of CLE simulations will produce the correct physics or, as suggested by random matrix theories, phase-quenched results.

We have performed some exploratory CLE runs at finite temperatures on $12^3 \times 6$ lattices, with m = 0.025 However, for 2-flavours and m = 0.025, we really need N_t large enough that $\beta = 5.6$ is on the low temperature side of the transition from hadronic/nuclear matter to a quark-gluon plasma, to have any chance of getting the correct physics. This means we would need $N_t \ge 12$. This situation is worse than that with 4-flavour QCD [19].

Because of the flavour ('taste') breaking for staggered quarks, it is possible that Wilson quarks would be better suited for CLE simulations of lattice QCD at finite μ . Other action modifications such as the inclusion of chiral 4-fermion interactions might produce better results.

We should mention methods which are being tried by other researchers to improve the performance of CLE simulations of QCD at finite μ . These include modifying the dynamics to include irrelevant terms which keep the unitarity norms closer to the SU(3) manifold [32], and including additional terms in the action, which improve the behaviour of the CLE, with coefficients that can be continued to zero afterwards [33].

Acknowledgments

Our simulations are performed on the Bebop cluster at Argonne's LCRC, Crays Cori and Edison at NERSC, the Stampede 2 cluster at TACC, the Bridges cluster at PSC, the Comet cluster at SDSC and Linux PCs belonging to the HEP division at Argonne.

References

- [1] G. Parisi, Phys. Lett. B 131, 393 (1983).
- [2] J. R. Klauder, Acta Phys. Austriaca Suppl. 25, 251 (1983).
- [3] J. R. Klauder, J. Phys. A 16, L317 (1983).
- [4] J. R. Klauder, Phys. Rev. A 29, 2036 (1984).
- [5] G. Aarts, E. Seiler and I. O. Stamatescu, Phys. Rev. D 81, 054508 (2010) doi:10.1103/PhysRevD.81.054508 [arXiv:0912.3360 [hep-lat]].
- [6] G. Aarts, F. A. James, E. Seiler and I. O. Stamatescu, Eur. Phys. J. C **71**, 1756 (2011) doi:10.1140/epjc/s10052-011-1756-5 [arXiv:1101.3270 [hep-lat]].
- [7] K. Nagata, J. Nishimura and S. Shimasaki, PTEP **2016**, no. 1, 013B01 (2016) doi:10.1093/ptep/ptv173 [arXiv:1508.02377 [hep-lat]].
- [8] J. Nishimura and S. Shimasaki, Phys. Rev. D **92**, no. 1, 011501 (2015) doi:10.1103/PhysRevD.92.011501 [arXiv:1504.08359 [hep-lat]].
- [9] K. Nagata, J. Nishimura and S. Shimasaki, Phys. Rev. D 94, no. 11, 114515 (2016) doi:10.1103/PhysRevD.94.114515 [arXiv:1606.07627 [hep-lat]].

- [10] G. Aarts, E. Seiler, D. Sexty and I. O. Stamatescu, JHEP **1705**, 044 (2017) doi:10.1007/JHEP05(2017)044 [arXiv:1701.02322 [hep-lat]].
- [11] E. Seiler, arXiv:1708.08254 [hep-lat].
- [12] G. Aarts, K. Boguslavski, M. Scherzer, E. Seiler, D. Sexty and I. O. Stamatescu, EPJ Web Conf. **175**, 14007 (2018) doi:10.1051/epjconf/201817514007 [arXiv:1710.05699 [hep-lat]].
- [13] G. Aarts and I. O. Stamatescu, JHEP 0809, 018 (2008) doi:10.1088/1126-6708/2008/09/018 [arXiv:0807.1597 [hep-lat]].
- [14] G. Aarts, L. Bongiovanni, E. Seiler, D. Sexty and I. O. Stamatescu, Eur. Phys. J. A **49**, 89 (2013) doi:10.1140/epja/i2013-13089-4 [arXiv:1303.6425 [hep-lat]].
- [15] G. Aarts, E. Seiler, D. Sexty and I. O. Stamatescu, Phys. Rev. D **90**, no. 11, 114505 (2014) doi:10.1103/PhysRevD.90.114505 [arXiv:1408.3770 [hep-lat]].
- [16] G. Aarts, F. Attanasio, B. Jäger and D. Sexty, JHEP 1609, 087 (2016) doi:10.1007/JHEP09(2016)087 [arXiv:1606.05561 [hep-lat]].
- [17] J. Langelage, M. Neuman and O. Philipsen, JHEP 1409, 131 (2014) doi:10.1007/JHEP09(2014)131 [arXiv:1403.4162 [hep-lat]].
- [18] D. Sexty, Phys. Lett. B **729**, 108 (2014) [arXiv:1307.7748 [hep-lat]].
- [19] Z. Fodor, S. D. Katz, D. Sexty and C. Török, Phys. Rev. D 92, no. 9, 094516 (2015) doi:10.1103/PhysRevD.92.094516 [arXiv:1508.05260 [hep-lat]].
- [20] K. Nagata, H. Matsufuru, J. Nishimura and S. Shimasaki, PoS LATTICE **2016**, 067 (2016) [arXiv:1611.08077 [hep-lat]].
- [21] Manuel Scherzer, poster presented at Lattice 2018, MSU, East Lansing, MI (2018)
- [22] D. K. Sinclair and J. B. Kogut, EPJ Web Conf. **175**, 07031 (2018) doi:10.1051/epjconf/201817507031 [arXiv:1710.08465 [hep-lat]].
- [23] J. Bloch, J. Glesaaen, J. J. M. Verbaarschot and S. Zafeiropoulos, JHEP **1803**, 015 (2018) doi:10.1007/JHEP03(2018)015 [arXiv:1712.07514 [hep-lat]].
- [24] K. Nagata, J. Nishimura and S. Shimasaki, JHEP **1607**, 073 (2016) doi:10.1007/JHEP07(2016)073 [arXiv:1604.07717 [hep-lat]].
- [25] E. Seiler, D. Sexty and I. O. Stamatescu, Phys. Lett. B 723, 213 (2013) [arXiv:1211.3709 [hep-lat]].
- [26] A. Ukawa and M. Fukugita, Phys. Rev. Lett. 55 (1985) 1854.
- [27] M. Fukugita, Y. Oyanagi and A. Ukawa, Phys. Rev. D 36 (1987) 824.
- [28] M. Fukugita and A. Ukawa, Phys. Rev. D 38, 1971 (1988).
- [29] K. M. Bitar et al., Phys. Rev. D 42, 3794 (1990).
- [30] F. R. Brown, F. P. Butler, H. Chen, N. H. Christ, Z. h. Dong, W. Schaffer, L. I. Unger and A. Vaccarino, Phys. Rev. Lett. 67, 1062 (1991). doi:10.1103/PhysRevLett.67.1062
- [31] W. Schaffer, Nucl. Phys. Proc. Suppl. 30, 405 (1993). doi:10.1016/0920-5632(93)90238-2
- [32] F. Attanasio and B. Jäger, arXiv:1808.04400 [hep-lat].
- [33] K. Nagata, J. Nishimura and S. Shimasaki, arXiv:1805.03964 [hep-lat].